

Supporting Information for:

Intelligent Nanomesh-Reinforced Graphene Pressure Sensor with Ultra Large Linear Range

Yancong Qiao^{1*}, Jinming Jian², Hao Tang¹, Shourui Ji², Ying Liu¹, Haidong Liu¹, Yuanfang Li¹, Xiaoshi Li², Fei Han³, Zhiyuan Liu³, Tianrui Cui², Guangyang Gou², Lelun Jiang¹, Yi Yang², Bingpu Zhou⁴, Tian-Ling Ren^{2*}, and Jianhua Zhou^{1*}

¹School of Biomedical Engineering, Sun Yat-Sen University, Shenzhen, 518107, China.

²School of Integrated Circuits (SIC) and Beijing National Research Center for Information Science and Technology (BNRist), Tsinghua University, Beijing, 100084, China.

³CAS Key Laboratory of Human-Machine Intelligence-Synergy Systems, Shenzhen Institutes of Advanced Technology, Chinese Academy of Sciences (CAS), Shenzhen 518055, China

⁴Joint Key Laboratory of the Ministry of Education, Institute of Applied Physics and Materials Engineering, University of Macau, Avenida da Universidade, Taipa, Macau 999078, China.

Email: zhoujh33@mail.sysu.edu.cn; rentl@tsinghua.edu.cn;
qiaoyc3@mail.sysu.edu.cn

Figure S1. The SEM image of the GO coated PU nanomesh.

Figure S2. The cross-section SEM image of the nanomesh-reinforced graphene.

Figure S3. The thickness of the nanomesh-reinforced graphene before compression measured by the profiler.

Figure S4. The height distribution of nanomesh-reinforced graphene before the compression.

Figure S5. The cross-section height distribution of nanomesh-reinforced graphene before the compression.

Figure S6. The nanomesh-reinforced graphene pulled by the force.

Figure S7. The nanomesh-reinforced graphene attached on the hand of tester for 10 hours.

Figure S8. Relative resistance variation of NRGPS on the PET substrate

Figure S9. Relative resistance variation of NRGPS as the function of the pressure.

Figure S10. Enlarged view of relative resistance variation of NRGPS during 990 to 1000 cycles.

Figure S11. The thickness of the nanomesh-reinforced graphene after compression measured by the profiler.

Figure S12. The height distribution of nanomesh-reinforced graphene after the compression.

Figure S13. The cross-section height distribution of nanomesh-reinforced graphene after the compression.

Figure S14. The pressure signals detected by the NRGPS under the table legs when the tester sat onto the table.

Figure S15. The pressure signals detected by the NRGPS under the table legs when placed a bottle onto the table.

Figure S16. The pressure signals detected by the NRGPS under the table legs when placed a mortar onto the table.

Figure S17. Schematic diagram of N-type MOSFET.

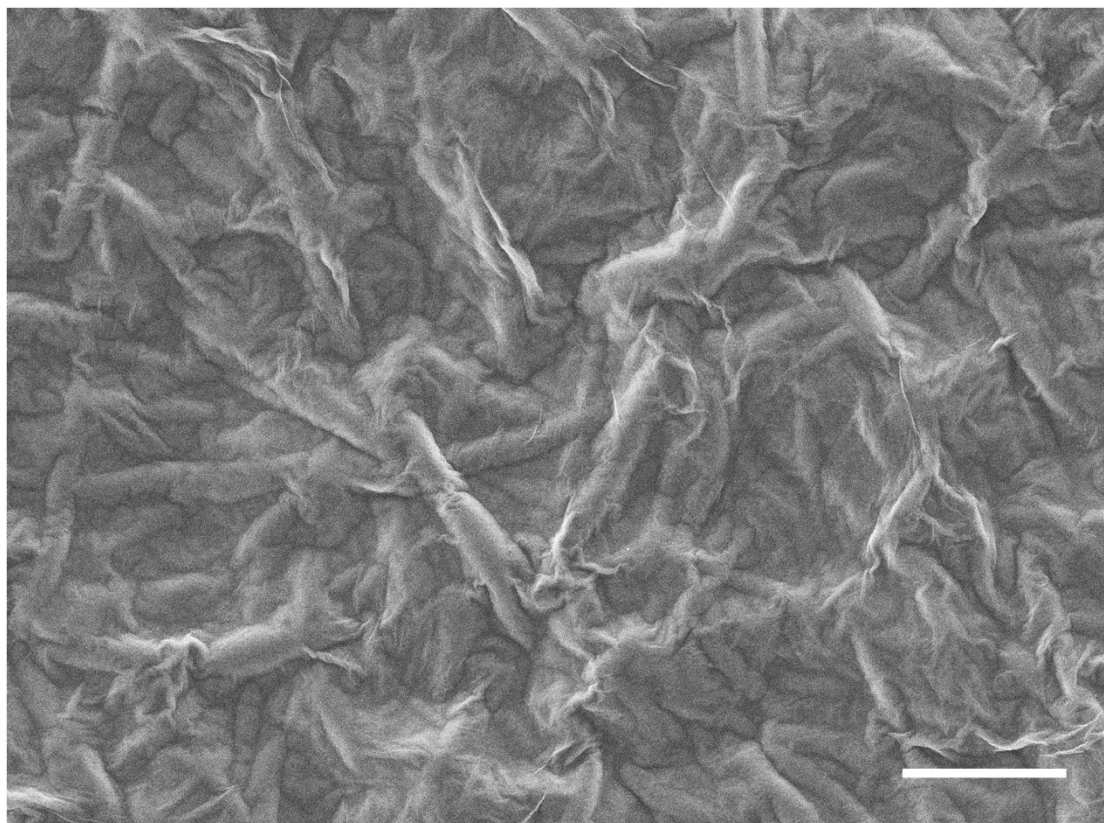


Figure S1. The SEM image of the GO coated PU nanomesh. The scale bar represents 20 μm .

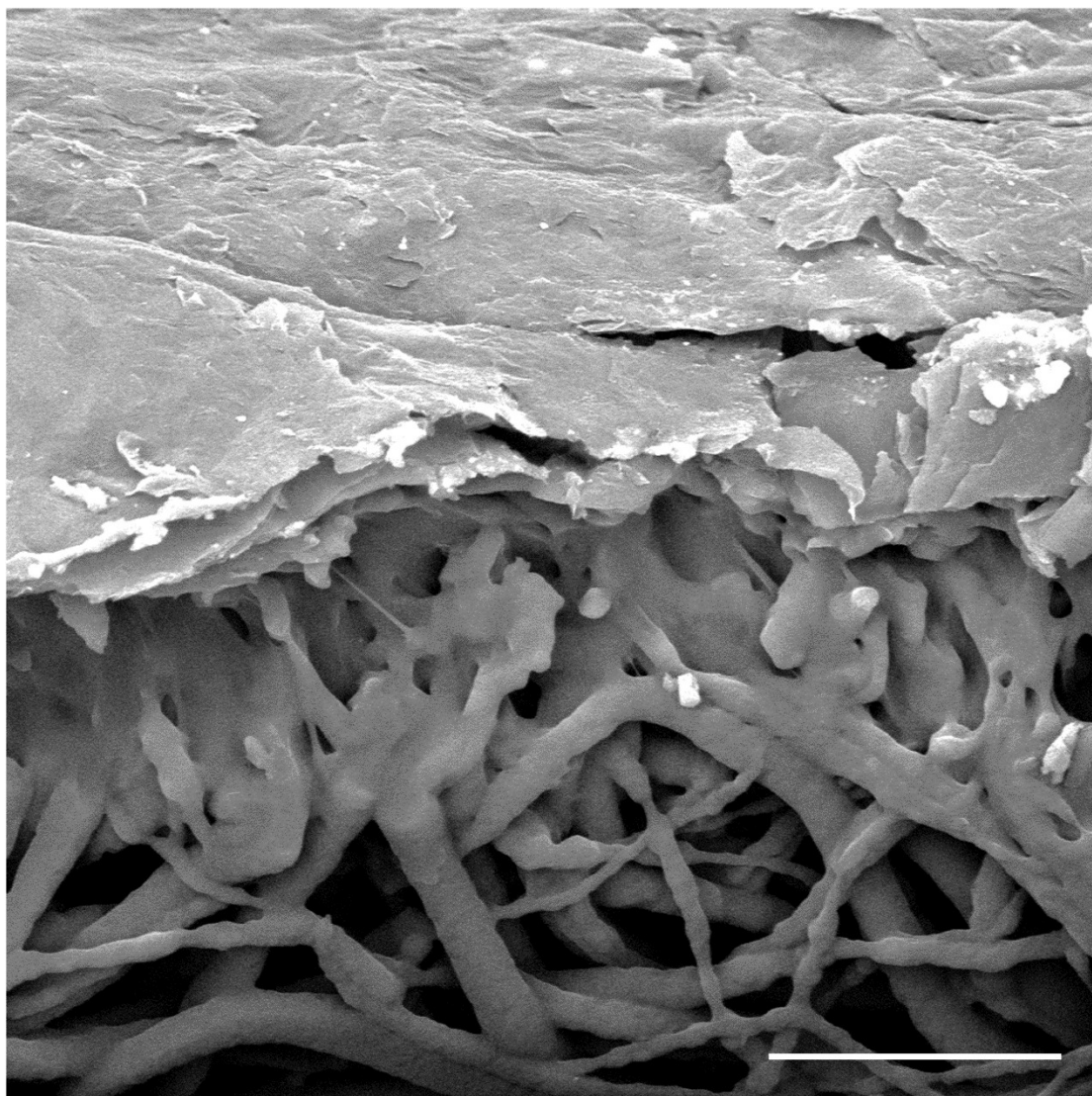


Figure S2. The cross-section SEM image of the nanomesh-reinforced graphene. The scale bar represents 10 μm .

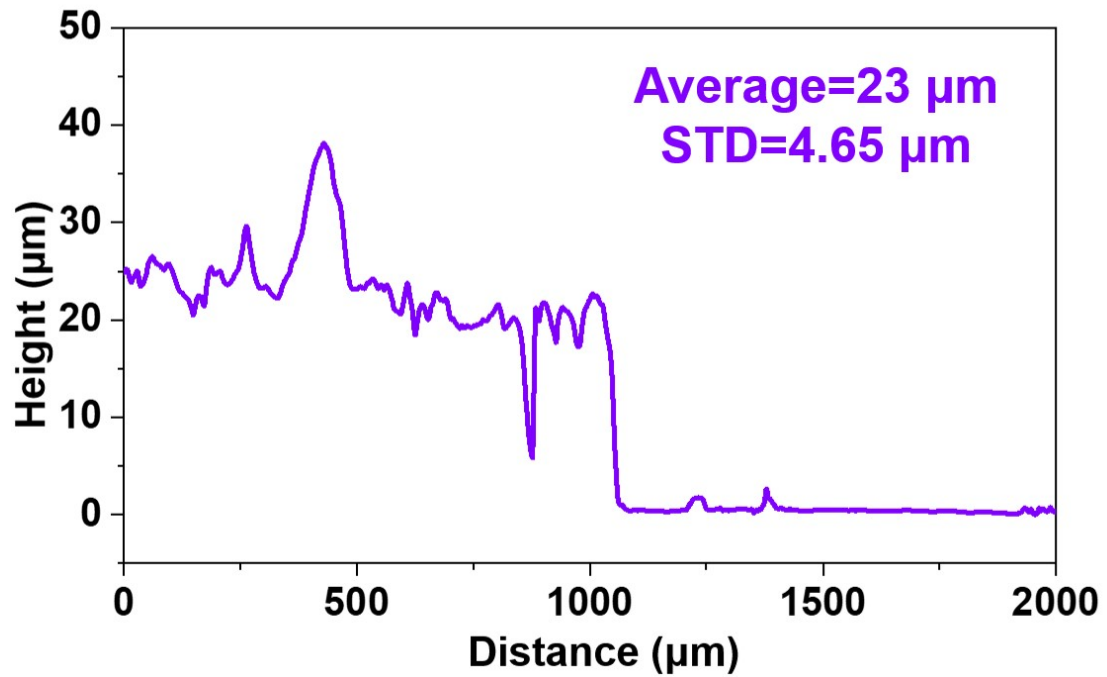


Figure S3. The thickness of the nanomesh-reinforced graphene before compression measured by the profiler.

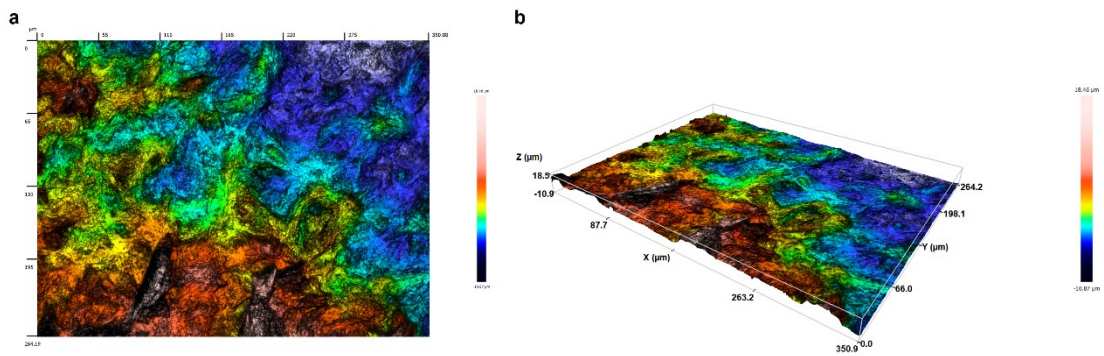


Figure S4. The height distribution of nanomesh-reinforced graphene before the compression. (a) 2D and (b) 3D image of height distribution of the nanomesh-reinforced graphene before the compression, measured by using a confocal microscope.

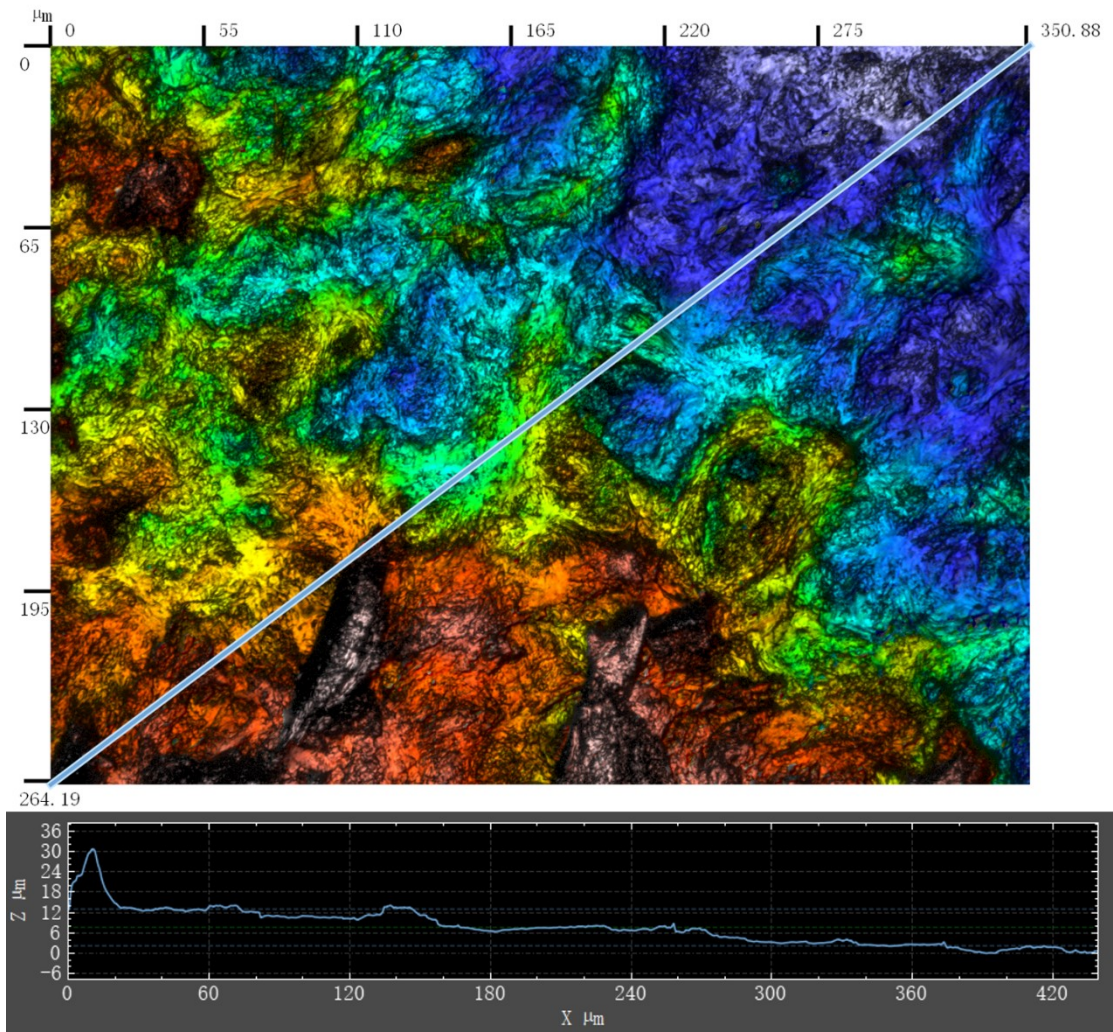


Figure S5. The cross-section height distribution of nanomesh-reinforced graphene before the compression.



Figure S6. The nanomesh-reinforced graphene pulled by the force of 0.2 N with the stress area of 0.28 cm².

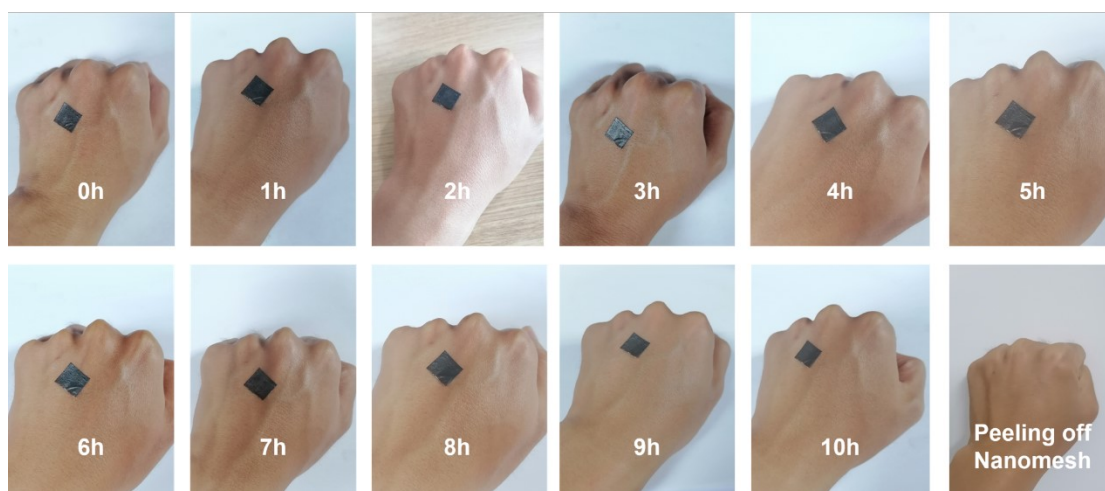


Figure S7. The nanomesh-reinforced graphene attached on the hand of tester for 10 h. After peeling off the nanomesh, the skin has no change.

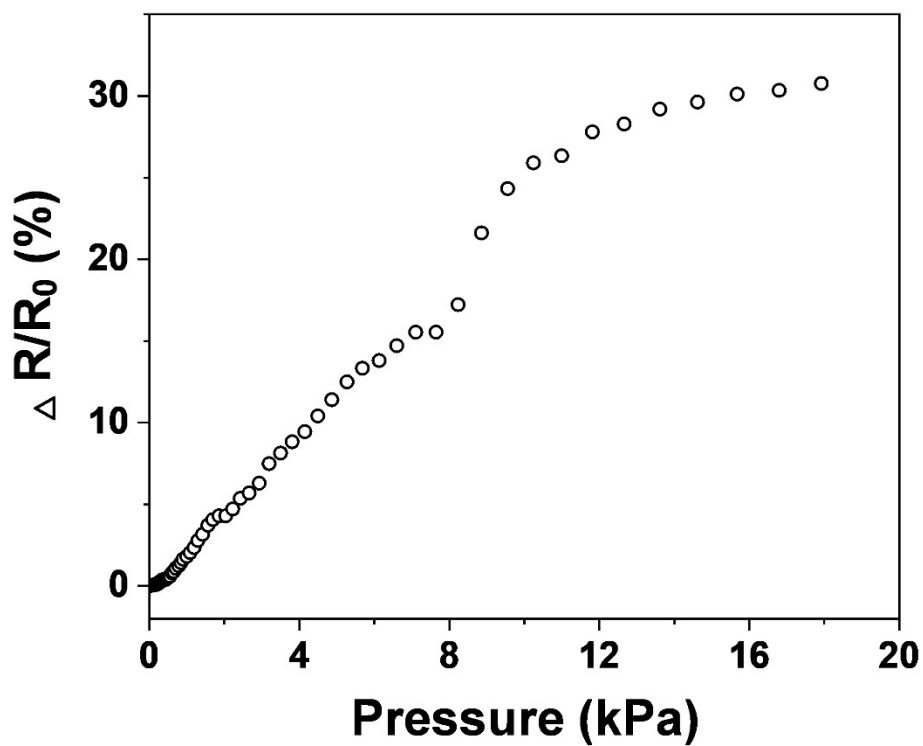


Figure S8. Relative resistance variation of NRGPS on the PET substrate and packaged by PDMS as the function of the pressure.

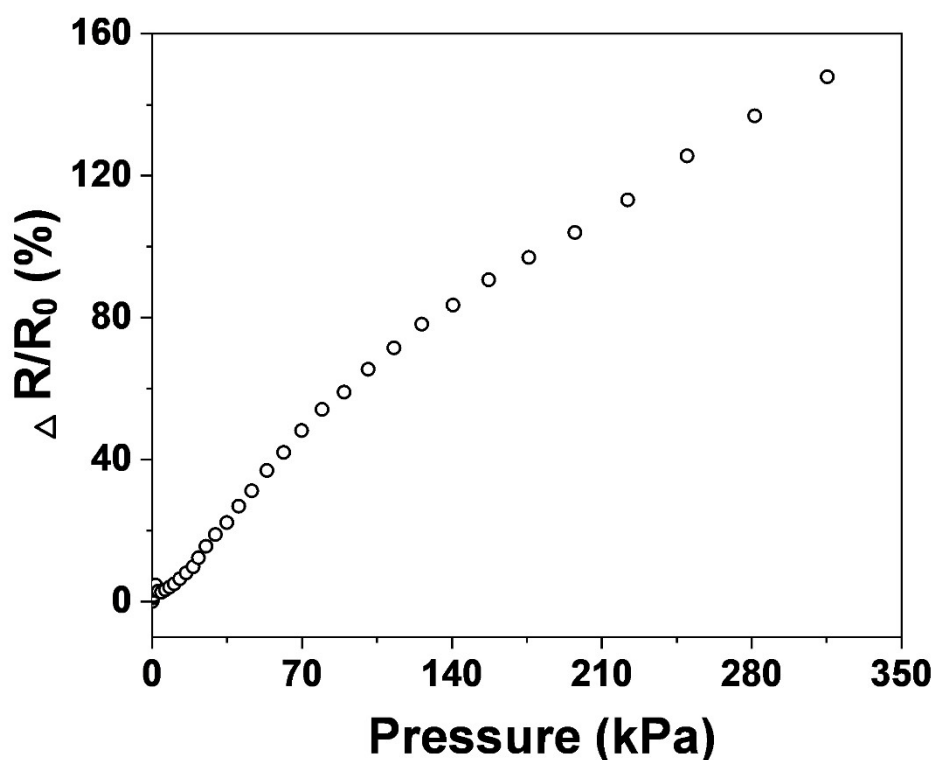


Figure S9. Relative resistance variation of NRGPS (reduced under the power density of 15 mW/cm^2) as the function of the pressure.

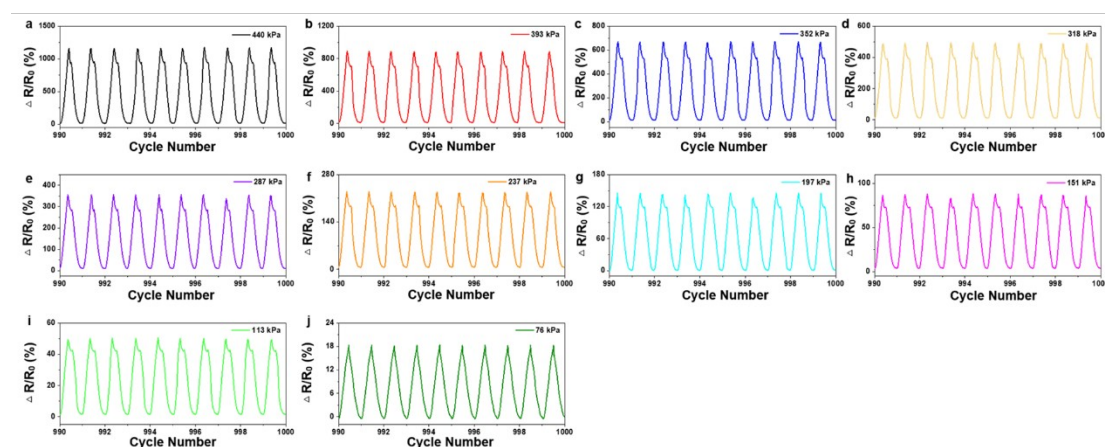


Figure S10. Enlarged view of relative resistance variation of NRGPS under repeated loading and unloading (990 to 1000 cycles) under different pressure of 76 kPa, 113 kPa, 151 kPa, 197 kPa, 237 kPa, 287 kPa, 318 kPa, 352 kPa, 393 kPa, and 440 kPa. During the beginning unloading process, the measuring equipment is a little unstable which leads to a vibration in the signals.

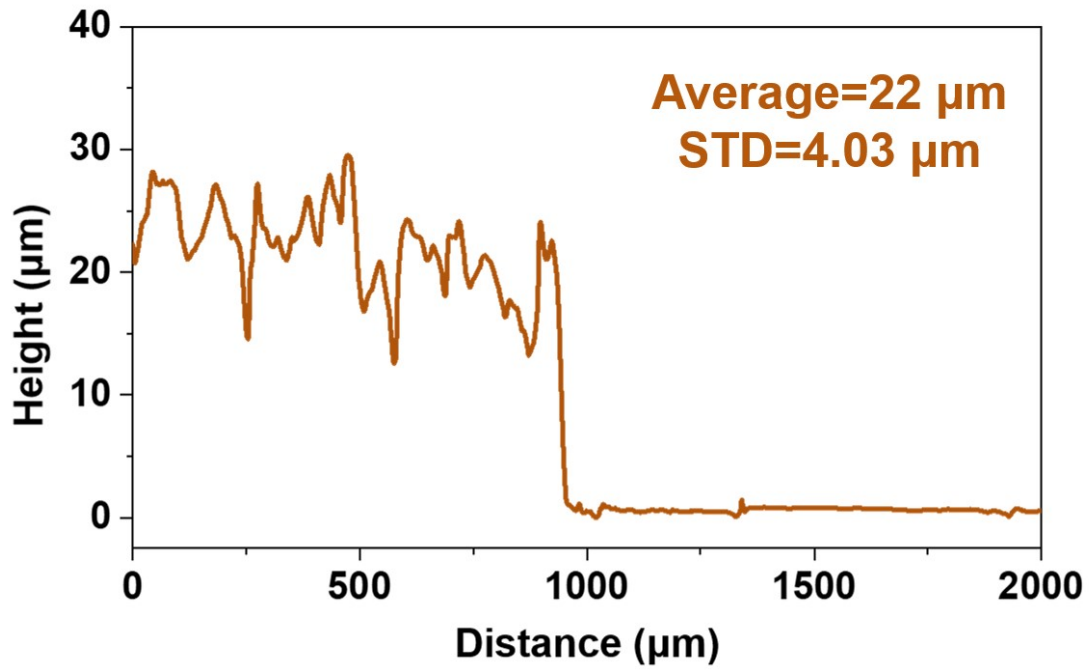


Figure S11. The thickness of the nanomesh-reinforced graphene after compression measured by the profiler.

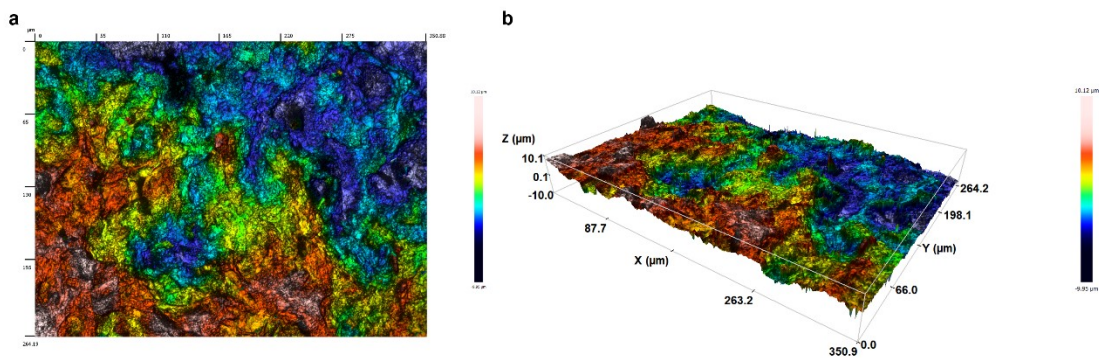


Figure S12. The height distribution of nanomesh-reinforced graphene after the compression. (a) 2D and (b) 3D image of height distribution of the nanomesh-reinforced graphene after the compression, measured by using a confocal microscope.

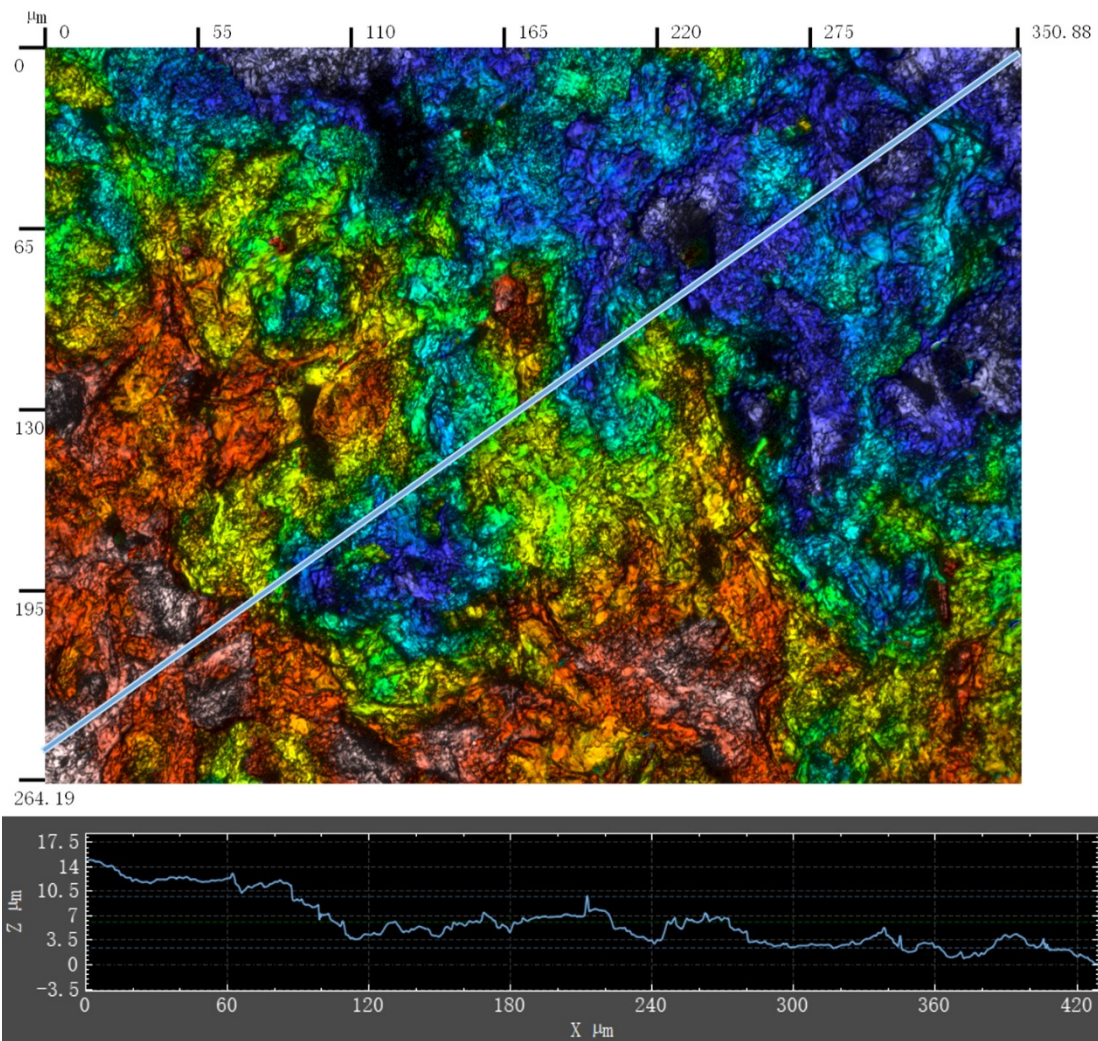


Figure S13. The cross-section height distribution of nanomesh-reinforced graphene after the compression.

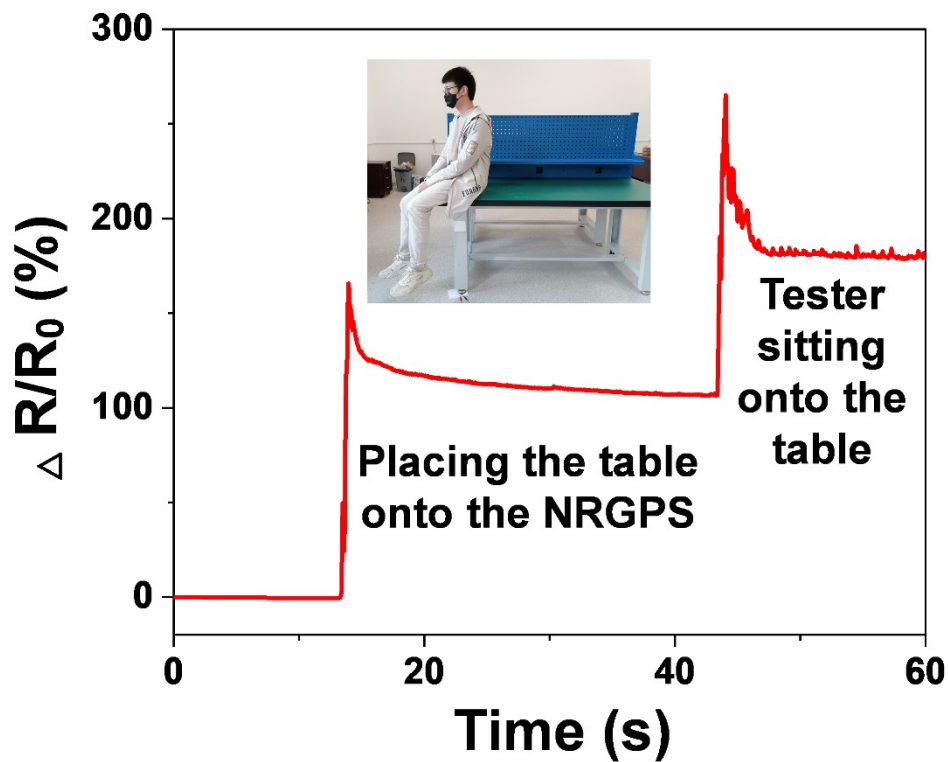


Figure S14. The pressure signals detected by the NRGPS under the table legs. After placing the table onto the NRGPS for 30 s, the tester then sat onto the table.

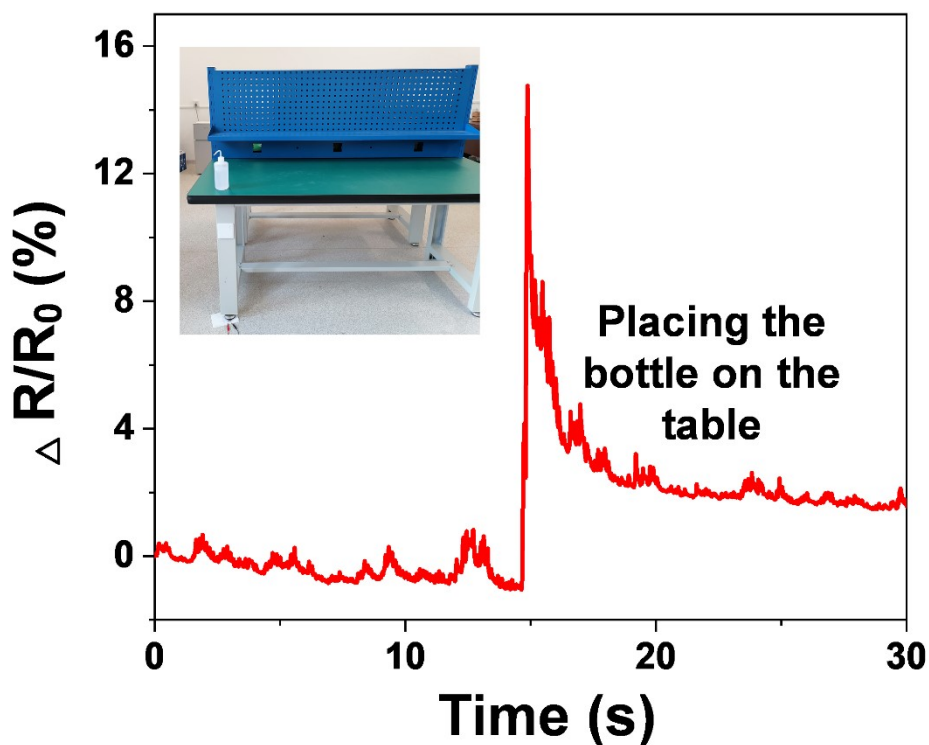


Figure S15. The pressure signals detected by the NRGPS under the table legs. A bottle containing ethanol (353 g) was placed onto the table.

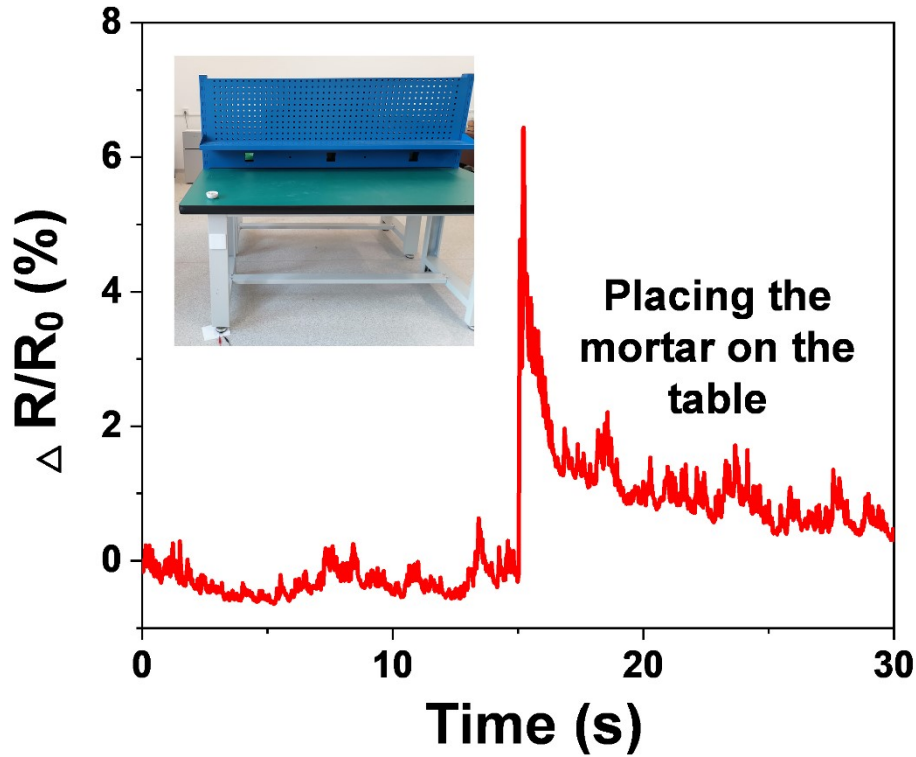


Figure S16. The pressure signals detected by the NRGPS under the table legs. A mortar (95.6 g) was placed onto the table.

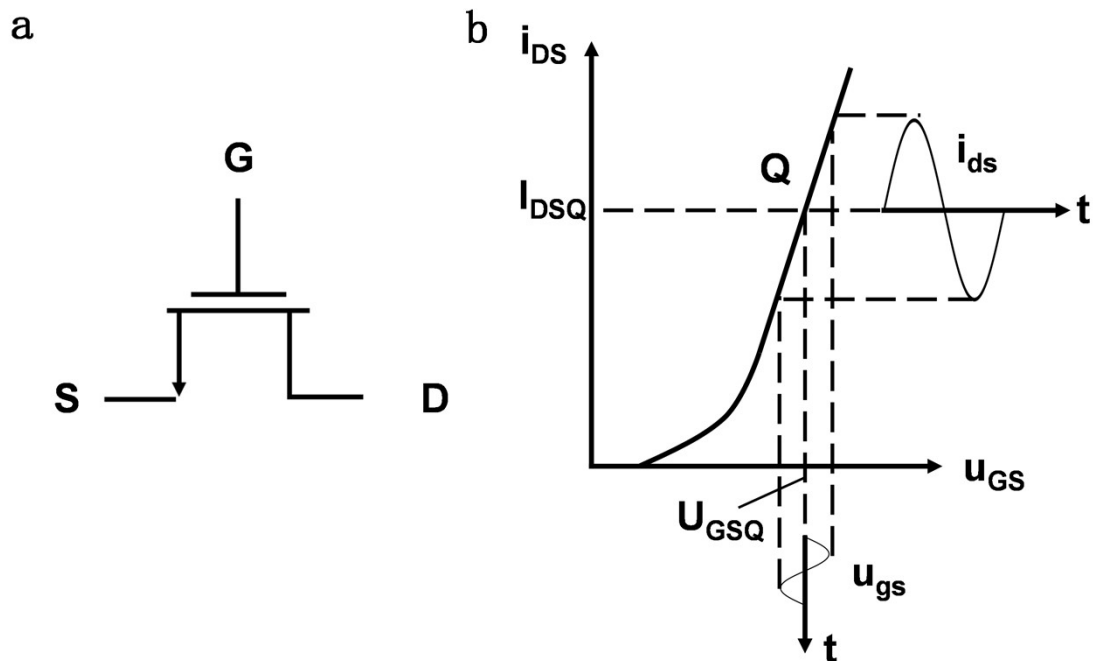


Figure S17. Schematic diagram of N-type MOSFET. (a) Schematic diagram of N-type MOSFET consists of gate (G), source (S), and drain (D). (b) Typical common source signal amplification curve of MOSFET.